





# Digital modelling as a tool for multidisciplinary study – the case of a rare sixteenth-century metallic globe

## Modelação digital como ferramenta para estudo multidisciplinar – o caso de um raro globo metálico quinhentista

PAULA REDWEIK<sup>1,2</sup>   
JOANA AMARAL<sup>3</sup>   
ISABEL TISSOT<sup>4\*</sup>   
FRANCISCO CHORRO-  
DOMINGUEZ<sup>5</sup>   
M. JOSÉ MARÍN-MIRANDA<sup>5</sup>   
SAMUEL GESSNER<sup>6,7</sup> 

1. Department of Earth Sciences and Energy, Faculdade de Ciências, Universidade de Lisboa, Campo Grande, 1749-016 Lisbon, Portugal
2. Instituto Dom Luiz, Faculdade de Ciências, Universidade de Lisboa, Campo Grande, 1749-016 Lisbon, Portugal
3. José de Figueiredo Laboratory – Museums and Monuments of Portugal, Rua das Janelas Verdes nº49, 1249-018 Lisbon, Portugal
4. LIBPhys-UNL, Department of Physics, Faculty of Science and Technology, NOVA University of Lisbon (NOVA-FCT), Caparica Campus, 2829-516 Caparica, Portugal
5. INTERRA - University Institute for Research into Sustainable Territorial Development, University of Extremadura Avenida de la Universidad, s/n, 10004 Cáceres, Spain
6. Interuniversity Centre for the History of Science and Technology, Faculdade de Ciências, Universidade de Lisboa, Campo Grande, 1749-016 Lisbon, Portugal
7. History of Astral Sciences, Laboratoire Temps Espace, Paris Observatory, 75014 Paris, France

\*isabelltissot@fct.unl.pt

### Abstract

While digital modelling of heritage objects has become standard practice, its multidisciplinary potential warrants greater emphasis. Using the case study of a rare Renaissance metallic celestial globe in Portugal, this article highlights the wide-ranging benefits of digitization across three key areas: historical research, conservation support, and public outreach. It underscores the importance of involving historians, digitization specialists, curators, and conservation professionals from the outset – both in prioritizing objects for modelling and in defining the criteria for digitization. The article advocates for a broad and inclusive perspective, encouraging awareness of the diverse disciplines that can benefit from digital models, whether in immediate applications or future research.

### Resumo

A modelação digital de objetos patrimoniais tornou-se uma prática amplamente difundida, mas o seu potencial multidisciplinar continua a exigir mais investigação. A partir do estudo de caso de um raro e valioso globo celeste renascentista em metal, existente em Portugal, este artigo evidencia as múltiplas vantagens da digitalização enquanto ferramenta de investigação histórica, apoio à conservação e promoção da divulgação pública. Destaca-se a importância de envolver, desde as fases iniciais do processo, historiadores, especialistas em digitalização, museólogos e conservadores – tanto na definição das prioridades de modelação, como na formulação dos critérios de digitalização. Defende-se, assim, uma abordagem abrangente e inclusiva, que promova a consciencialização para a diversidade de disciplinas que podem beneficiar dos modelos digitais, seja em contextos de aplicação imediata ou em investigações futuras.

### KEYWORDS

3D modelling  
Scientific instruments  
History of science  
Preventive conservation  
Public engagement

### PALAVRAS-CHAVE

Modelação 3D  
Instrumentos científicos  
História da ciência  
Conservação preventiva  
Mediação cultural

## Introduction

The study and conservation of scientific instruments have gained growing attention in recent years, with research being undertaken in various fields to explore the material culture of such instruments [e.g., 1-2]. However, further methodological development is needed to ensure the preservation of this heritage, which is characterized by a unique set of material and functional specificities [3-4]. Scientific instruments embody the practices of science and education, evident in their materials, construction, and functionality – and, perhaps most revealingly, in the marks of use and wear they accumulate over time.

The dual nature of scientific instruments – encompassing both material technology and intangible elements like gestures and modes of scientific use – demands interdisciplinary methodologies. To ensure comprehensive preservation, these approaches must integrate historical research, material analysis, and conservation practices. While notable progress has been made [e.g., 5-6], further research is needed to establish a truly holistic approach. Recent efforts have focused on developing integrated documentation methods for scientific instruments [7] and refining examination techniques that consider their specific material and functional characteristics, such as mechanical components and surface coatings [8]. Comparable methodologies have been applied to related heritage objects, including industrial engines [9] and kinetic art [10]. Additional research has focused on wear characterization [11] and innovative conservation techniques [12].

Many of these instruments are difficult or impossible to handle due to size, fragility, or significance, limiting physical analysis. Additionally, instruments with exceptionally large or minuscule dimensions present challenges in obtaining a comprehensive visual and global assessment. To overcome these limitations, the application of advanced study tools such as 3D scanning and modelling offers a promising solution. These technologies are already widely used in cultural heritage for dissemination and communication [13]. More recently, they have been employed for historical study and conservation monitoring in fields such as, for example, paintings, sculptures, and archaeology [e.g., 14-16]. Despite their potential, their application to the study and conservation of scientific heritage remains underexplored.

Although 3D scanning and modelling are not new techniques, this study proposes a distinct and integrated approach that utilizes accessible equipment and software, both user-friendly and relatively low-cost. One key advantage of these tools is their ability to capture extensive information before and during conservation and restoration processes, enabling detailed object analysis without causing harm. This accessibility makes them especially valuable for documenting and studying fragile, remote, or otherwise difficult-to-access objects.

### The Schissler Globe as a case study

The Schissler Globe, a rare sixteenth-century metallic celestial globe, exemplifies a complex and historically significant scientific instrument that remains difficult to access. Its scientific and historical value makes it an ideal case study for exploring how 3D scanning and modelling can aid historical research, conservation, and public engagement. The Globe was produced in 1575 in one of the most renowned workshops for mathematical instruments in Augsburg, Germany. The craftsman Christoph Schissler the Elder (c. 1531-1608) created numerous and various instruments, such as compasses, geometric squares, and astronomical compendia [17]. Many of these were intended for nobles interested in the mathematical arts. The time of the Globe's arrival in Portugal remains unclear, but by the late monarchy, it embellished King D. Carlos's private library at the Palácio das Necessidades. In 1956, it was selected for permanent display at the Palácio Nacional de Sintra, where it remains. Its significance was first noted by António Estácio dos Reis [18-19] and later Gessner showed how it was linked to Caspar Vopel's 1536 globe [20].

A celestial globe is a spherical model of the sky that depicts the visible star constellations as seen from the centre of the Earth. Traditionally, such globes were used to simulate the apparent

motion of fixed stars and the Sun, both above and below the horizon, when suitably mounted in a stand. Globes can represent and explain the variation of the length of day and night at different terrestrial latitudes and across different seasons of the year. Using their various scales, one can determine sunrise and sunset times, the azimuth of a star's rising, and many more things.

With 42 cm in diameter the Schissler Globe is among the larger metallic globes surviving from the sixteenth century [21]. Its surface is composed of twelve copper gores, riveted or screwed onto a skeleton made of circular metal bands. The hollow structure is traversed by an iron axis forming its centre. Tilted with respect to this axis, at approximately 23.5 degrees, at opposite points of the Globe, two axes extend outward and suspend the Globe within a meridian ring. The entire surface of the Globe, along with the meridian ring, is engraved and gilded [22]. The engravings feature the classical constellations, canonical since antiquity, with corresponding labels as well as a couple of constellations introduced in the sixteenth century. Several bright individual stars are given with their names, such as Vega, Arcturus, and Spica, along with the principal celestial circles used in astronomy, such as the celestial equator and the ecliptic, the tropic and arctic circles. Several components that were originally part of the structure are now missing: the hour circle and its index, which allowed the rotation of the Globe to be tracked, and the horizontal ring with its stand, on which the Globe was originally placed.

## Towards the creation of a multidisciplinary analytical tool

### Preliminary tests for the digitalization of the Globe

The core of our approach consisted in the digitisation of the Globe using near-range photogrammetry and multiview automation. Various setups were tested to ensure a complete, high-quality, well-framed photographic coverage of the sphere. Due to the Globe's fragility, value, and permanent display at the Palácio Nacional de Sintra, initial testing was conducted with two dummy globes. The first test, carried out in diffuse indoor lighting, showed that fixing the camera on a tripod and rotating the globe produced better results than moving the camera. A need for higher-resolution imaging was also identified. However, two additional challenges had to be overcome in the case of the Schissler Globe: the absence of its original stand and surface deformation that restricted rotation within the meridian ring. To overcome these, a custom support had to be designed to stabilize and safely rotate the Globe during photography.

In a second phase, we used a dummy globe of the same diameter *in situ* at the Palácio Nacional de Sintra and tested a support frame built from available materials in coordination with conservation staff. The setup – two stacked tables, wooden bars, and screws (Figure 1) – was designed to ensure stability and safe imaging. Foam panels surrounding the table helped to diffuse light, minimize reflections and optimize the visibility of engraved lines as dark lines on a light background. The Globe remained secure throughout and all components were fully reusable, with minimal, reversible modification. The final imaging was conducted employing three LED panels in a sunlight-free room, ensuring both image quality and the Globe's preservation (Figure 1b).

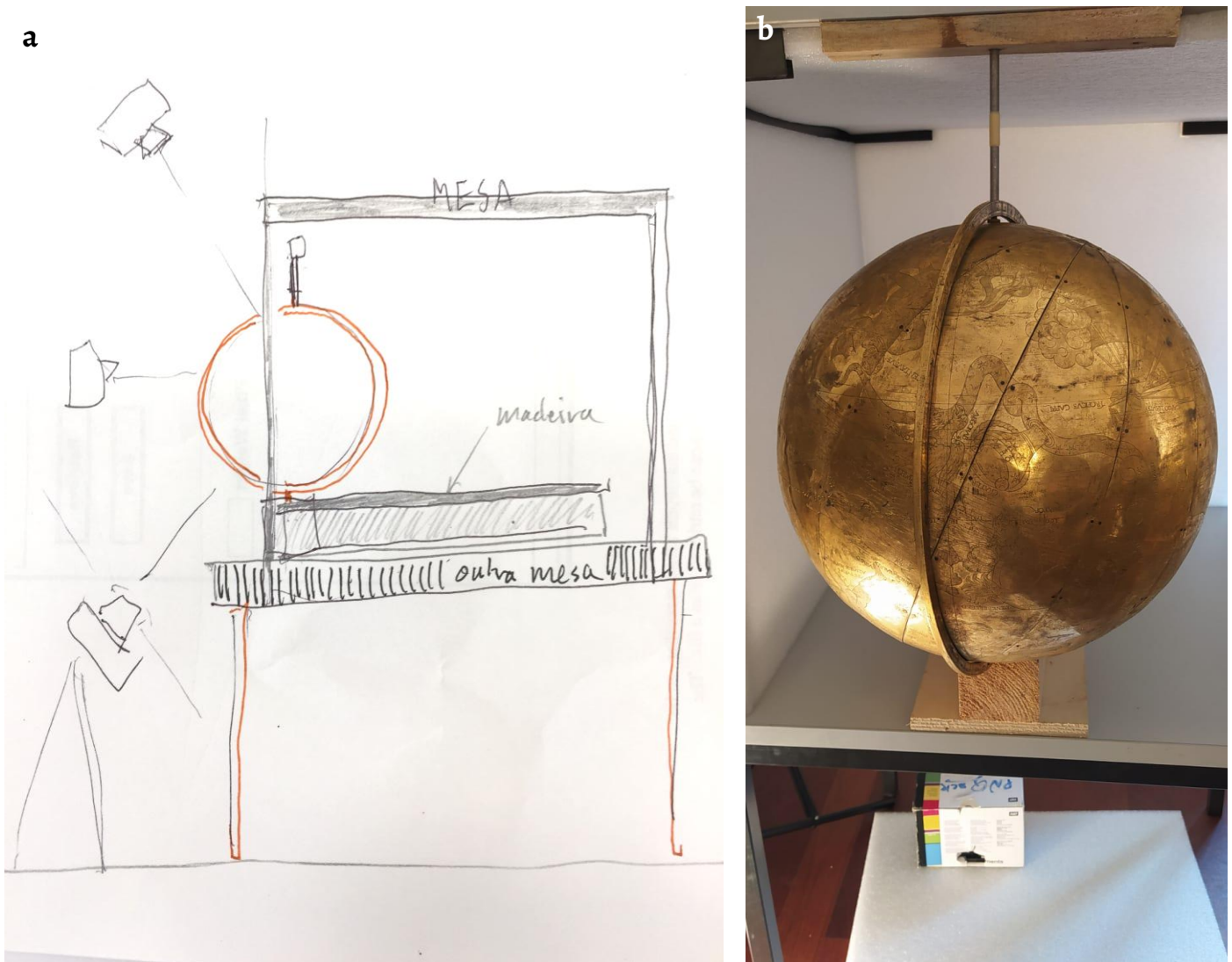


**Figure 1.** Support for the Globe: a) design sketch; b) Schissler Globe inserted in the support.

### Image acquisition

Preliminary tests had shown that three fixed camera positions – aligned with the equator, Arctic, and Antarctic circles – provided full surface coverage with sufficient image overlap. At each position, the Globe was rotated  $15^\circ$  around its North-South axis between shots, producing 25 images (the last overlapping the first). Because part of the surface was obscured by the meridian ring the conservator decided to remove it and a fourth image set was taken (Figure 2). For this last set, the Globe rested on a torus-shaped cushion with its axis in horizontal position. For the first three sets, the Globe rotated around its own iron axis; for the fourth, the cushion was rotated. This approach ensured the Globe's surface remained unstressed throughout.

We used a 50 Mpixel Canon EOS 5DSR camera controlled through an application on laptop computer via a USB cable. Aperture, exposure, and object distance were kept constant while changing the camera position for each image set. It was crucial that these parameters remained unchanged for all photographs also within each set. The object distance was about 47 cm (to the nearest point on the Globe) in all sets. Remote control triggered the shutter to avoid vibrations, thereby ensuring maximum image sharpness.

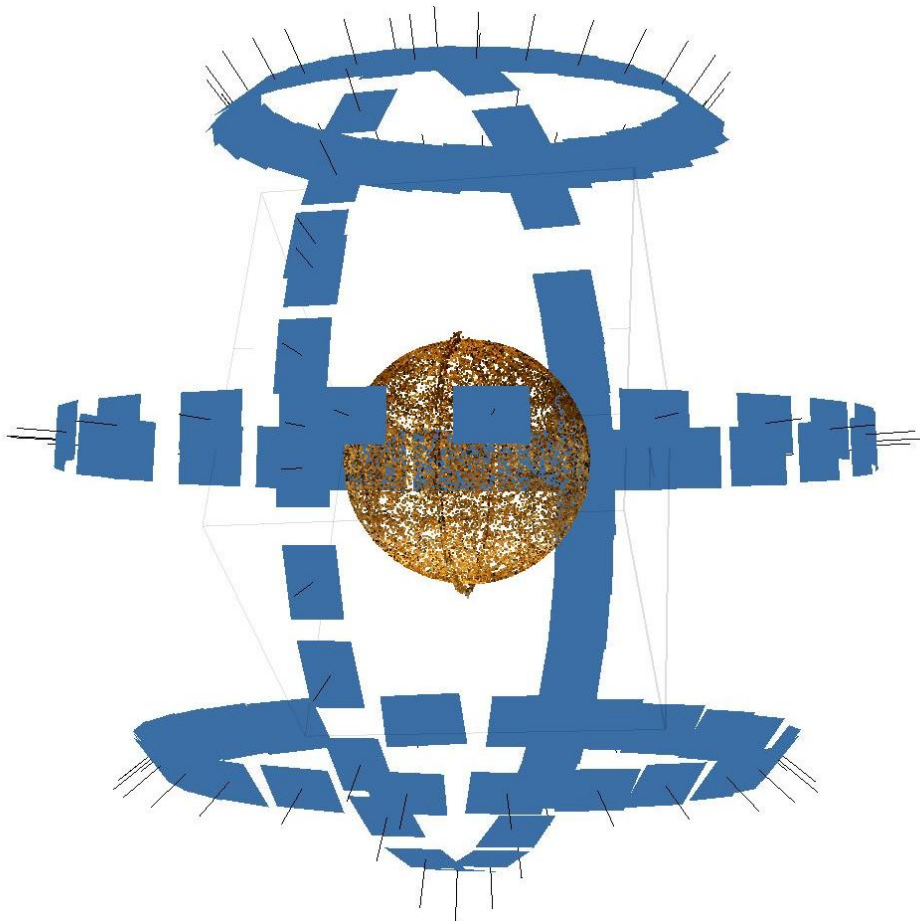


**Figure 2.** Virtual configuration of the photographic sets around the Globe. The vertical series of picture planes corresponds to the fourth set, covering the area previously hidden behind the meridian ring.

## Photogrammetric: processing

### *Image masking and alignment*

The 145 photographs taken under slightly varying lighting conditions were processed by the software Agisoft *Metashape* (v1.6.1) [23] to create a 3D model. Initial processing was disrupted by surrounding elements like table legs despite using white foam panels to neutralize the background.

As a workaround, masks were applied to exclude all elements beyond the Globe. The camera setup with four fixed positions required only four different masks as it allowed the reuse of one single mask per position. Each one was manually created in Adobe Photoshop [24], saved as an alpha channel in one reference image, and imported into *Metashape* for batch application across the corresponding set. After masking, the photographs were aligned in *Metashape*, which automatically calculated their relative orientations. With extraneous elements masked, *Metashape* used only Globe's features to determine camera positions and orientations. This created the virtual setup shown in Figure 2, simulating a stationary Globe with a moving camera.

### *Point cloud and mesh*

Based on successful photo alignment a dense point cloud could be generated by intersecting 3D rays from matching points across images (Figure 3). The surface details are very clear, and the Globe's geometry is accurately reconstructed without relying on colour. The point cloud is complete and the surface irregularities match those of the original. A lighter band in the point cloud model appears in the area lying behind the meridian ring. The colour variation there is due to different lighting affecting the fourth image set. Despite this variation, a mesh was then created and textured with high-resolution images, producing a detailed 3D model of the Globe.



**Figure 3.** Dense point cloud obtained from the photogrammetric coverage.

### ***Defining a coordinate system***

Since the point cloud and mesh lack inherent scale, the model was scaled in Agisoft *Metashape* [23]. Radiography and tomography studies [22] showed that the Globe's inner skeleton has an internal iron axis between the ecliptic poles. These ecliptic poles therefore offer the most stable reference points. The known 420 mm diameter between the poles was used to scale the model. A 3D coordinate system was then defined using three reference points: the ecliptic North Pole (ECNP), South Pole (ECSP), and the vernal point (ARIES). Each reference point was identified in at least three images, and their average 3D positions were used to define coordinates (in mm): ECNP = (0, 0, 210), ECSP = (0, 0, -210), and ARIES = (210, 0, 0), the origin representing the Globe's estimated centre. The X-axis passes through ARIES, the Z-axis aligns with the ecliptic poles, and the XY-plane defines the ideal ecliptic plane (Figure 4).

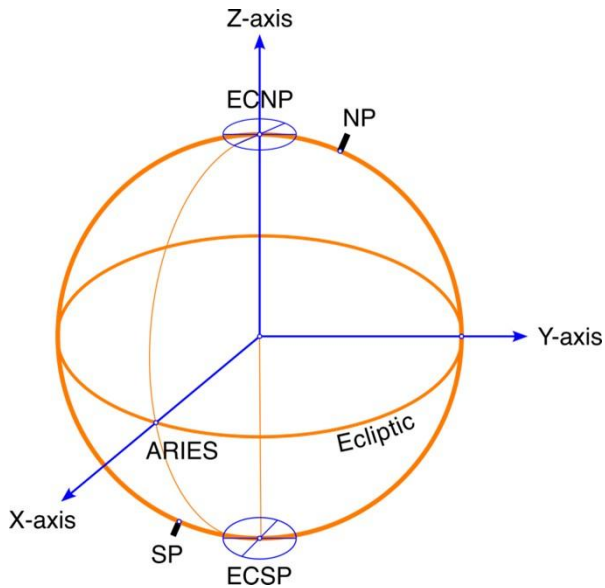


Figure 4. 3D coordinate system defined for the Globe.

### Deformations imaging

That the Globe cannot freely rotate within its meridian ring is due to deformation which occurred at some point after its manufacture. It is more likely due to a deformation of the spherical shape rather than of the meridian ring whose cross section makes it very solid. Our analysis therefore focused on the geometry of the Globe's surface. Any deviation from an ideal spherical form was treated as deformation. To assess this, *CloudCompare* [25] (v2.13 alpha) was used as the primary tool. First, a 420 mm reference sphere was created in *CloudCompare* using the *Primitive Factory* tool and centred on the origin of the previously defined coordinate system. The dense point cloud with the same centre was then imported. The *Cloud-to-Primitive* tool in *CloudCompare* calculated the distances between all the points and the ideal sphere – thus quantifying surface deformations. Analysing the histogram of the distances we were able to readjust the diameter of the sphere so that the most populated bin became the one with zero distance (less than 1  $\mu\text{m}$ ). The adjusted diameter was calculated as 421.107 mm. This way we created a sphere that privileges the undeformed Globe points. We deliberately disregarded the deformations when making this diameter adjustment, therefore not applying a least squares best fit method. We introduced a colour scale to the results to facilitate interpretation: red and orange indicate negative deviations (inward deformations), white represents neutral areas (no deviation or small deviation), and green to blue signify positive deviations (outward bulging of the surface). This process yielded two digital reproductions of the Schissler Globe: a high-resolution textured 3D model capturing surface details and inscriptions, and a deformation model showing deviations from a ca. 420 mm ideal sphere. Both are complete, highly detailed, and geometrically precise – even fine chisel marks are visible. With the exception of the meridian ring, the scaled textured 3D model can serve as a true digital twin, offering valuable support for research and outreach as will be shown in the sections below.

### The tool in action

Thanks to these digital models, the Globe can be analysed from multiple disciplinary perspectives, employing either the textured model or the deformations model, as appropriate. The examples discussed here range over three distinct disciplinary fields: historical research, conservation, and public dissemination.

### Reading Schissler’s practices through star positions

Celestial globes are mathematical instruments that, among other functions, provide an overview of stellar constellations and yield star positions. An inscription on the Globe refers explicitly to the adjustment of the engraved positions in accordance with the precession of the equinoxes: “The stars of this globe were numbered and distributed according to the motion of the eighth sphere and adjusted to our times and year of 1575”. The maker reveals, however, neither the source of the stellar coordinates nor the method by which the precession correction has been obtained. An earlier study based on only four stars near the ecliptic [21], showed a match between the Globe’s longitudes and the Copernican precession value. The high-resolution 3D model now allows measurement of many more stars, enabling a more sophisticated study comprising three aspects: comparison with various star catalogues available to the maker, estimating the precession value applied, and possible systematic errors due to Schissler’s craft procedure to position the stars.

The task involves identifying stars on the Globe and measuring their XYZ coordinates from the 3D model, which are then converted into angular ecliptic coordinates. This transformation enables direct comparison with historical star catalogues and provides a basis for estimating the amount of precession calculated and applied by Schissler for the year 1575. In order to produce a meaningful estimation, it is essential to consider several factors affecting accuracy: the precision of the historical catalogue data, the accuracy of Schissler’s engraving, and the positional fidelity of our measurements derived from the digital model. For this preliminary study, fifteen labelled stars of first or second magnitudes, and distributed across the Globe were selected (Figure 5). From the textured 3D model Cartesian XYZ coordinates were obtained through a triangulation via least squares adjustment between measurements on all photographs on which the star was well visible, performed by *Metashape* software [23].

A MATLAB routine [26] converted the Cartesian coordinates into ecliptic latitude ( $\beta$ ) and longitude ( $\lambda$ ) by using the following Equations 1-2:

$$\beta = \sin^{-1} \frac{Z}{\sqrt{X^2+Y^2+Z^2}} \quad (1)$$

$$\lambda = \tan^{-1} \frac{Y}{X} \quad (2)$$

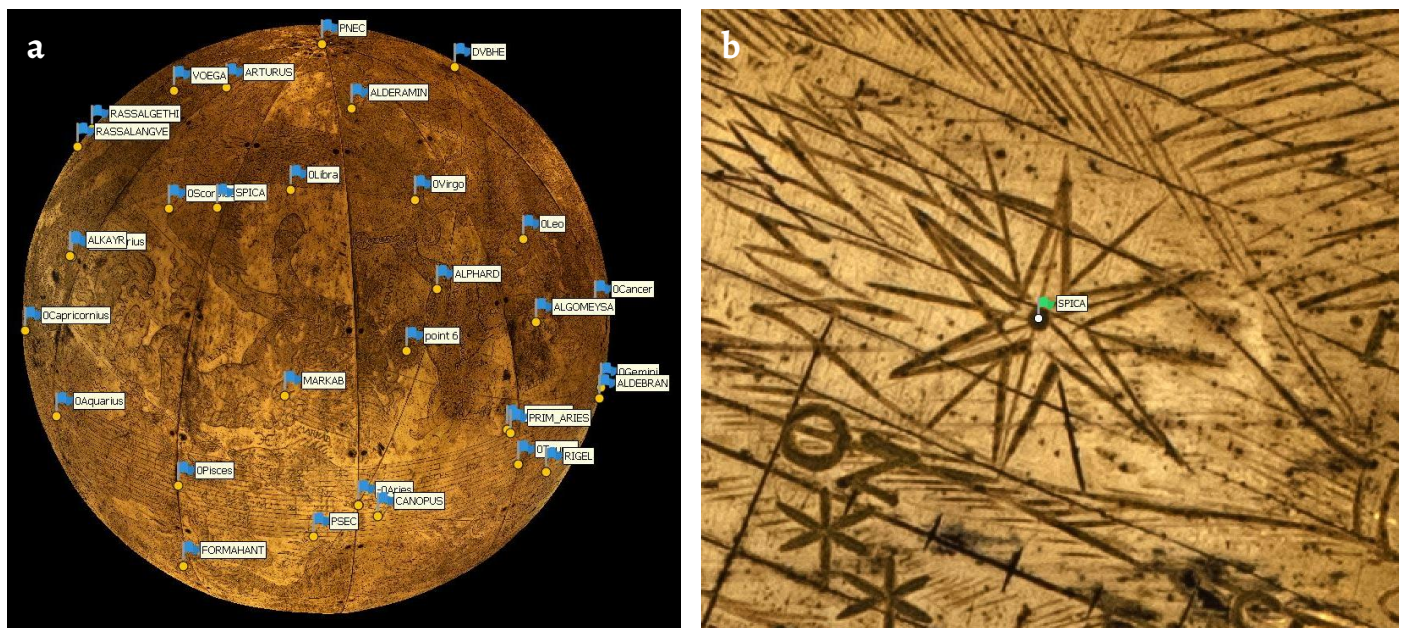


**Figure 5.** Schissler Globe: a) selected stars used to estimate the precession correction used by Schissler, along with the zero points of the zodiac signs marked on the 3D model; b) measurement of the star Spica Virginis on a single photograph, providing input for the least squares triangulation (based on all measurements on photographs on which the star was well visible) to estimate its spatial position within the 3D model.

Each star measured on the Schissler Globe was compared with historical catalogues Schissler may have accessed. This study, being still in a preliminary phase, focuses on two: Ptolemy's catalogue (Toomer's 1984 edition based on Greek manuscripts [27]) and Copernicus' *De Revolutionibus* (1543) [28] (Table 1). While the Globe's inscription states that its stars were adjusted to 1575, both the source of coordinates and method of adjustment are to be determined.

**Table 1.** The set of fifteen selected stars for which ecliptic latitude ( $\beta$ ) and longitude ( $\lambda$ ) were measured, listed in order of decreasing latitude. Stars are identified by the labels found on the Globe. The subscript *P* or *C* references Ptolemaic resp. Copernican values; the index *i* runs through the stars used. Weighted deviations –cf. Equation 4–  $\Delta_{iP}^w$  of over  $\frac{1}{2}^\circ$  are marked in bold.

Engraved star name		Latitude $\beta$	Longitude $\lambda$	Shift $\zeta_P$ [°] w/r Ptolemy 1984	Weighted $\Delta_{iP}^w$	Shift $\zeta_C$ [°] w/r to Copernicus 1543	Weighted $\Delta_{iC}^w$
ALDERAMIN	$\alpha$ Cep	68.54	6.54	19.88	<b>0.41</b>	26.54	<b>0.35</b>
VOEGA	$\alpha$ Lyr	62.08	278.49	21.16	-0.07	27.82	-0.15
DVBHE	$\alpha$ UMa	48.84	127.75	20.08	<b>0.61</b>	23.75	<b>2.47</b>
RASSALGETHI	$\alpha$ Her	37.55	248.79	21.12	-0.09	27.79	-0.23
RASSALANGVE	$\alpha$ Oph	36.00	255.95	21.21	-0.17	27.78	-0.22
ARCTURUS	$\alpha$ Boo	32.52	197.96	20.96	0.04	27.63	-0.10
ALKAYR	$\alpha$ Aql	29.29	294.80	21.07	-0.06	27.64	-0.11
MARKAB	$\alpha$ Peg	19.39	347.48	20.81	0.18	27.48	0.03
SPICA	$\alpha$ Vir	-2.58	197.57	21.17	-0.16	27.57	-0.06
ALDEBRAN	$\alpha$ Tau	-5.45	63.46	20.79	0.21	27.46	0.05
ALGOMEYSA	$\alpha$ CMi	-16.37	110.29	21.12	-0.11	27.79	-0.27
ALPHARD	$\alpha$ Hya	-20.44	141.04	21.04	-0.03	27.71	-0.19
RIGEL	$\beta$ Ori	-31.82	70.71	20.98	0.03	28.21	<b>-0.60</b>
ALHABOR	$\alpha$ CMa	-39.26	99.05	21.38	-0.29	28.05	<b>-0.42</b>
CANOPUS	$\alpha$ Car	-74.92	100.05	22.88	<b>-0.49</b>	29.55	<b>-0.53</b>
Weighted average shift $\bar{\lambda}$				21.01*		27.51*	
Variance				0.074		0.059**	

\*The average longitude shift  $\bar{\lambda}$  is calculated by weighing the values by the cosine of latitude ( $\cos \beta$ ) of the star.

\*\*Variance for the Copernican longitudes without the outlier "DUBHE".

Table 1 presents one method to estimate the average longitude shift ( $\bar{\lambda}$ ) as an approximation of the correction presumably applied by the Globe's maker.  $\bar{\lambda}$  is obtained from the difference between the measured longitude ( $\lambda$ ) of each selected star on the Globe and its catalogued longitude ( $\lambda_{\text{cat}}$ ), expressed as  $\zeta = \lambda - \lambda_{\text{cat}}$ . To obtain a meaningful average (Equation 3), these differences are weighted according to the star's latitude:

$$\bar{\lambda} = \frac{\sum_i \zeta_i \cos \beta_i}{\sum_i \cos \beta_i} \quad (3)$$

This is justified, since manufacturing errors in longitude near the poles translate into proportionally larger angular deviations [29]. Similarly, to get an estimate of the overall closeness of a given catalogue with the engraved star positions, we evaluate the variance of the applied shift. Here all (unweighted) differences  $\Delta$  between the measured longitudes ( $\lambda$ ) and the shift-updated positions ( $\lambda_{\text{cat}} + \bar{\lambda}$ ) are analysed. Since the error is expected to increase with

latitude, weights based on the cosine of the latitude ( $\cos \beta_i$ ) are introduced (Equation 4) to account for this effect:

$$\Delta_i^w = (\zeta_i - \lambda) \cos \beta_i \quad (4)$$

The weighted variance is then the sum of the squares of these differences  $\Delta_i^w$  divided by the number of stars minus 1. When comparing the weighted deviations  $\Delta_i^w$  of individual stars, anomalies are readily identified. The variance is lower with respect to Copernicus' catalogue, which suggests that this is a likely source for the Globe's star positions. Nevertheless, the star Dubhe stands out as an outlier relative to Copernicus' data, while its deviation from Ptolemy's values resembles that of the other stars. As we cannot exclude manufacturing lapses or occasional interventions by Schissler, isolated outliers were not included in such statistical analysis. Moreover, examining the full set of stars reveals that those with deviations exceeding  $\frac{1}{3}^\circ$  are all located north of  $48^\circ$  or south of  $31^\circ$  ecliptic latitude. This pattern points to a possible systematic error in longitude that grows with increasing distance from the ecliptic. Such systematic discrepancies could plausibly originate from the mechanical process used to mark the stars on the Globe.

Finally, regarding the underlying precession theory, the average difference in longitude between the values in different catalogues and the Globe's positions – explicitly adjusted for 1575 – must be examined. More research is needed in that respect because various different hypotheses about Schissler's procedure still need to be tested. For now, the consistent fit of star Dubhe's longitude as given in Ptolemy (1984 edition, based on Greek manuscripts) in contrast with its deviation of near  $2^\circ 30'$  when compared with Copernicus or even with Ptolemy's sixteenth-century print editions can serve as a marker. So, while Ptolemy's catalogue could serve as the basis for star positions, the longitude shift applied to it remains to be explained. Ptolemy's precession of  $1^\circ$  per century does not fit the numbers. Alfonsine precession theory (e.g. using a star catalogue with the Alfonsine epoch of 1 June 1252) would amount to a longitude shift of  $20^\circ 19'$ : nearly  $1^\circ$  less than what we measured. This difference of ca.  $1^\circ$  for many globes after 1550 has been noted by Dekker [30]. Indeed, based on the chosen stars of the Schissler Globe, the Copernican precession theory provides a better fit. Specifically, the average longitude shift of approximately  $27^\circ 30'$  relative to Copernicus' catalogue is very close to Copernican precession theory, which stipulates a shift of  $27^\circ 49'$ . This finding corroborates the preliminary conclusion reached by Gessner [21]. One observes, however, that the deviations of Schissler's star positions from Copernicus' values are scattered by about  $\frac{1}{3}^\circ$  (standard deviation derived from the variance). The near-exact correspondence reported in Gessner [21], based on only four stars, was coincidental while the present result, based on more stars, better represents the realities of globe manufacture. A clear path for future research emerges. Including a larger set of stars and incorporating additional historical star catalogues may uncover further characteristic outliers, show systematic 'error' patterns, potentially linked either to Schissler's mechanical method for marking star positions on the Globe or to the particular source catalogue he employed.

### How did Schissler build the Globe? Construction and material analysis

The analysis of the Globe allows furthering our understanding of Schissler's craftsmanship and of his manufacturing process. The detailed 3D model offers comprehensive access to the surface features enabling both thorough documentation and study of the construction – and this without direct physical access to the Globe itself. As mentioned above, the Globe is composed of twelve gilt copper gores fixed by rivets on top of a metallic frame. The centre points of the stars were punched, and inscriptions, constellation figures, stars, and celestial circles were engraved and chiselled into the surface. Subsequently the spherical copper plates were fire-gilded using mercury gold alloy technique [22].

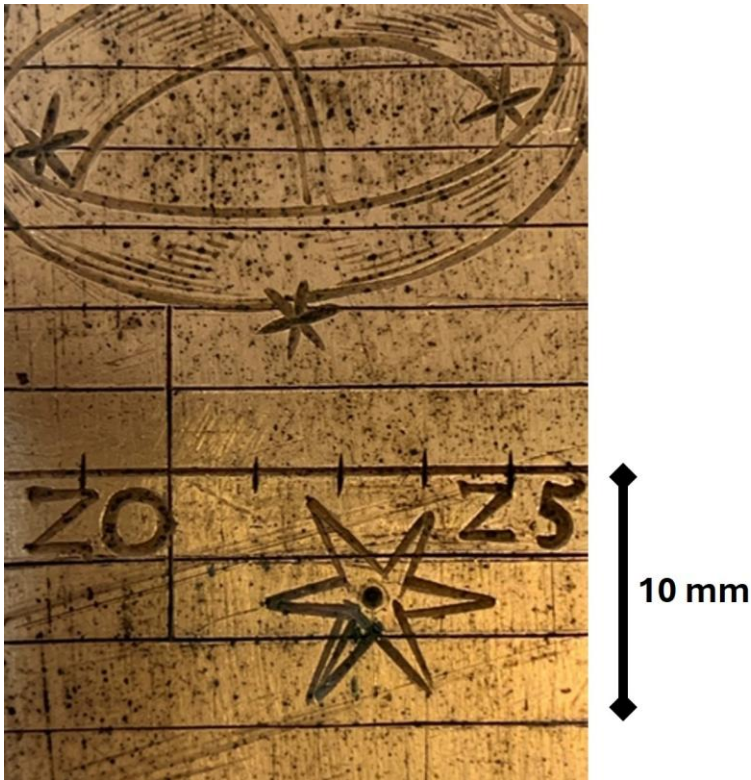


**Figure 6.** Detail of the engraved and chiselled inscriptions on the Globe, revealing aspects of the manufacturing process, especially the sequence of inscriptions. Shown is a portion of the sign of Scorpio, the scale of the ecliptic and some stars of the constellation Libra.

By combining 3D modelling with high-resolution photography, a detailed analysis of the decorative process becomes possible. It reveals the sequential order in which the elements were inscribed. For example, as shown in [Figure 6](#), intersecting lines indicate that the ecliptic was traced first, followed by vertical line markings in its scale, the constellation figures, the numbering, and finally the stars themselves. Before the stars were fully depicted, the centre of the larger ones was initially marked with a punch. Additionally, visible corrections and refinements were identified: for instance, in [Figure 6](#), the large star south of the ecliptic shows overlapping lines suggesting that one line was retouched after the others. This analysis offers valuable insight into the artisan's working technique, enabling comparisons with methods of other craftsmen and offering a deeper understanding of the visual language and craftsmanship behind the Globe. Such observations are rendered particularly easy through digital modelling – rather difficult to attain extensively without permanent access to the Globe.

The digital modelling also enables studying deformations linked to the Globe's construction technique. For example, [Figure 7](#) highlights deformation in the North Pole area where the ends of the gores are attached to the top of the pole by rivets. Around each rivet, inward deformations (revealed by red colour) occur ranging from approximately  $-0.5$  to  $-1.0$  mm, corresponding to the mechanical stresses induced by fixing the metal plates in place. Similar deformations can be seen alongside other fixations of the gores. Additionally, the plate areas adjacent to the top fixations exhibit distortions relative to the ideal sphere, resulting from the tension required to bend and hold the gores at the poles. Recognizing these manufacturing-related deformations is crucial, as the accumulated tension from fixation pressure may lead to progressive structural alterations over time.

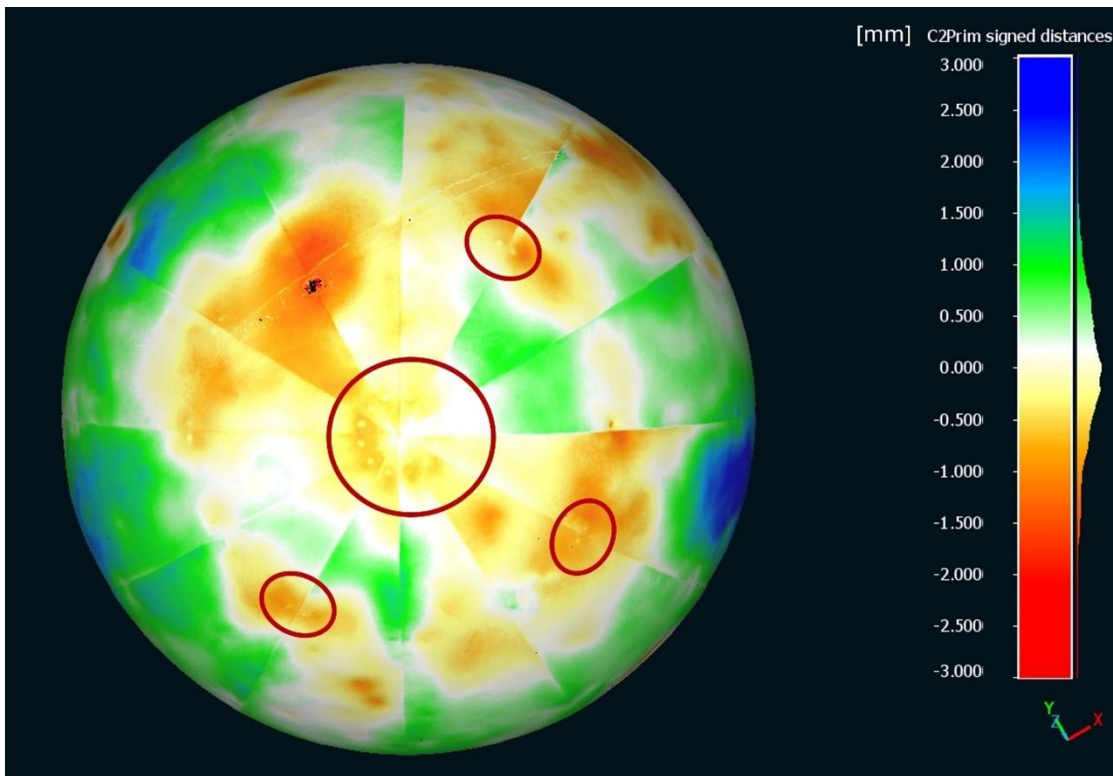


**Figure 7.** Deformation mapping of the ecliptic North Pole region. Red circles highlight the areas with rivets where the plates are fixed to the structure. Adjacent plate areas show deformation due to the tension required to bend and secure them at the poles.

### How does it look like today? Conservation analysis

One of the most valuable applications of digital modelling lies in preventive conservation, offering a quantitative basis for monitoring the Globe's physical state over time. By establishing a detailed 3D reference model at a specific moment, subsequent scans can be systematically compared to detect subtle changes such as wear, cracking, or surface corrosion. This capability transforms conservation from a reactive to a proactive practice, enabling the identification of early-stage deterioration. Importantly, the detection of deformations related to original manufacturing stresses – such as localized tension in certain areas – provides critical information for adjusting environmental and display conditions to mitigate further mechanical strain. Such targeted interventions can reduce the risk of exacerbating damage, including the formation of cracks or permanent distortions.

Figure 8 presents a good example of this potential by mapping deformations around the Globe's ecliptic South pole. A notable inward deformation of approximately  $-2$  mm is to be observed in an extensive region. It is not attributable to manufacturing processes. Further investigation revealed that this deformation resulted from prolonged static loading, as the Globe had been resting on a support directly beneath this pole for an extended period. Although the copper plates have a considerable thickness (estimated between 1.5 and 2.0 mm), the cumulative weight of the Globe (around 7 kg) caused material fatigue and deformation under sustained pressure. This case study underscores how digital modelling can uncover otherwise hidden conservation risks and inform necessary modifications to display and handling protocols to better preserve such artifacts.

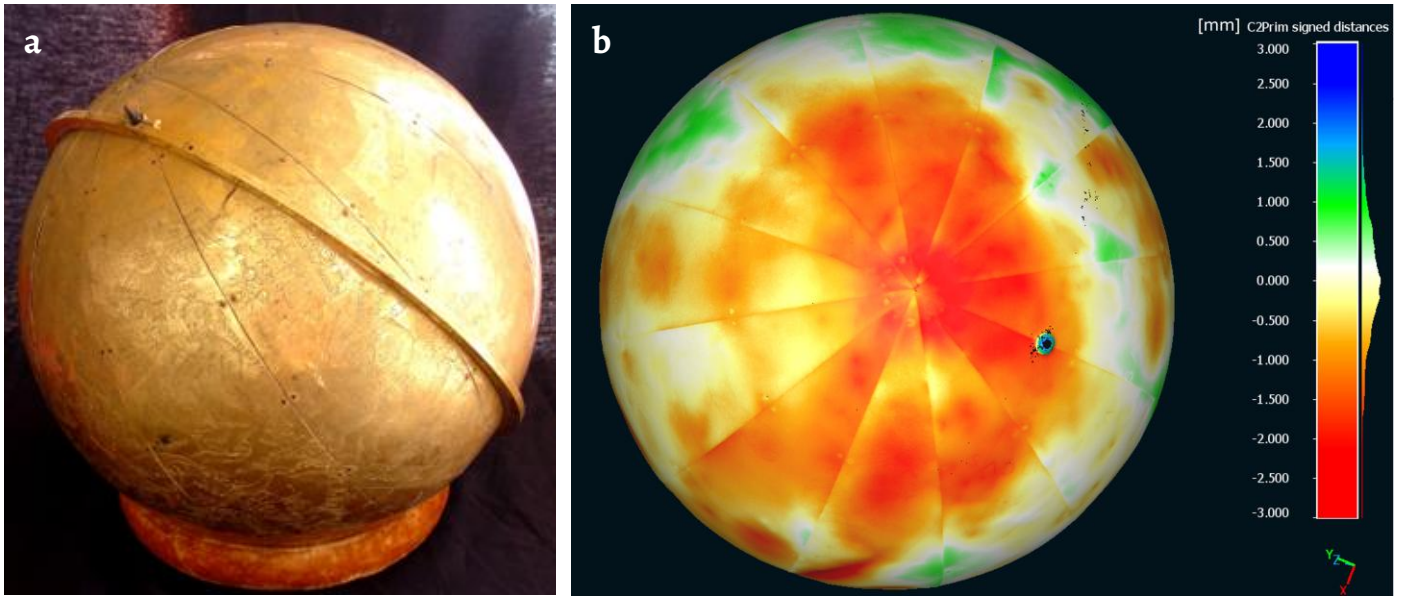


**Figure 8.** The Globe displayed on a torus shaped base cushion, with its entire weight resting near the southern ecliptic pole (a). The deformation model shows inward deformations caused by prolonged exhibition in this position (b).

### The Schissler Globe for all

A key application of the Globe's digital twin is to provide free and universal access to this important heritage object through the internet. This channel can be used for enhancing its dissemination and public engagement. To achieve this, the 3D textured model has been integrated into an interactive web application (<http://bit.ly/3ZLBIOS>) developed on the ArcGIS Online platform [31] (Figure 9). The application opens with an introductory page summarizing the Globe's general and historical context. Users can then navigate to a 3D viewer that allows full exploration of the Globe – rotating, zooming, and panning in any direction.

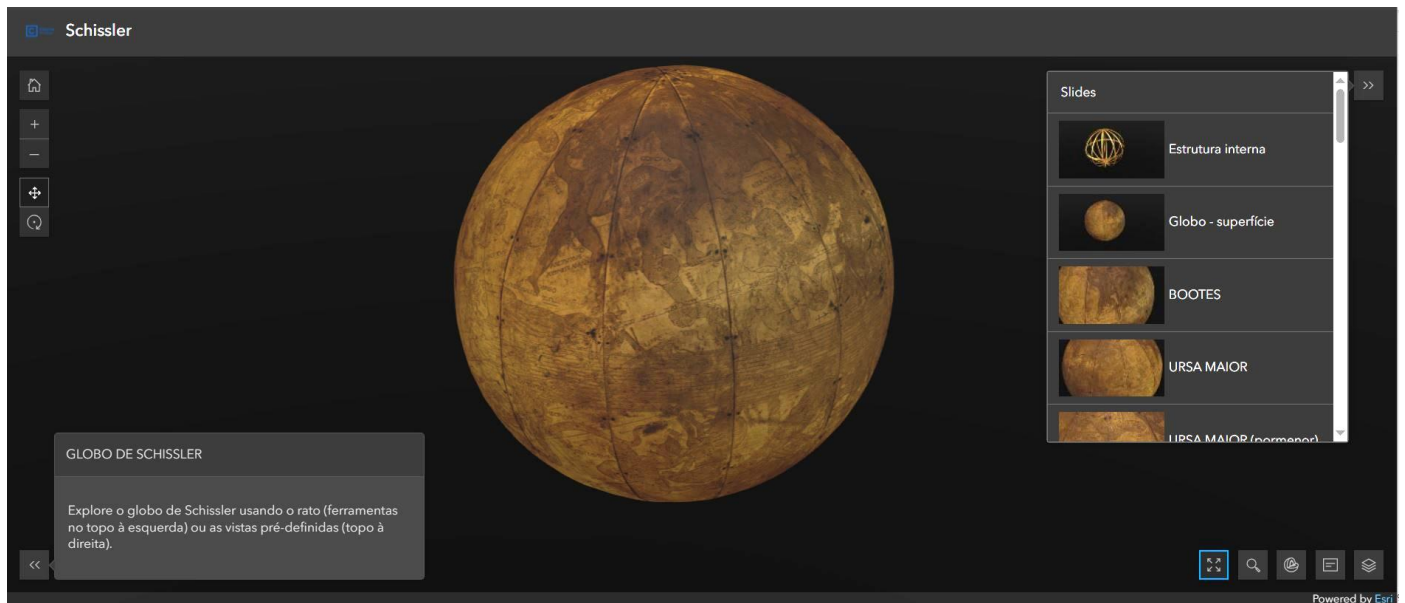


**Figure 9.** Screenshot of the web application based on ArcGIS Online. Exploring page of the developed application. On the right side, the structure of the guided tour. On the left side the navigation commands. On the bottom right, app commands: magnifying (an additional zoom by means of a virtual magnifying glass), slicing (to see the interior structure), return to the info page and layer selection.

The platform is designed to provide an engaging guided tour, highlighting the celestial Globe's interior structure, gilded surface, and key constellations. Additionally, users can interactively click on any location on the Globe's surface to access pop-up windows containing detailed information about the principal constellation or feature in that area. To maintain web performance and responsiveness, a reduced-resolution 3D model is employed within the viewer. However, each pop-up includes a direct link to an original high-resolution photograph of the corresponding region, opening in a separate window. This feature is a simple way to allow detailed examination of the Globe's surface at a resolution exceeding that of the 3D model itself. The original photographs, intended primarily for an expert audience such as conservators and researchers, offer approximately 30 % higher resolution than the sub-millimetre accuracy of the 3D model. In the central areas – those nearest the camera during image capture – the pixel size corresponds to roughly 0.06 mm on the actual object. This dual-level access balances usability for general audiences with the detailed analytical needs of specialists, ensuring the Globe's visual and structural intricacies are accessible to a broad spectrum of users.

## Conclusions

This study demonstrates the transformative impact of digital modelling on the research, preservation, and public engagement of historical scientific instruments, as exemplified by the case of Christoph Schissler's sixteenth-century celestial Globe. The creation of a high-resolution 3D digital twin yielded three major outcomes: it enables detailed historical analysis of star positions and manufacturing techniques; it supports conservation by detecting surface deformations; and it enhances accessibility through an interactive web platform designed for both experts and the general public. Handling and imaging a fragile, reflective metallic object poses a challenge. The project's success relied on close coordination with conservation professionals thorough the preparation of the photographic environment, and maintaining fixed camera positions under controlled lighting to avoid visual artifacts. These measures ensured the object's safety while enabling high-quality data capture. Multiview photogrammetry software was instrumental not only in reconstructing the 3D model but also in defining a precise internal coordinate system. With external control points unavailable due to display constraints, spatial referencing was achieved using three distinct features on the Globe. This allowed for accurate scaling and orientation, culminating in both a textured model and a deformation map that visualizes deviations from an ideal sphere – essential tools for future research and preservation.

Importantly, the study lays the groundwork for future work in multiple directions. The historical analysis will benefit from expanding star position measurements to include a broader selection of stars, allowing for comparisons with various historical catalogues such as those of Ptolemy, the Alfonsine Tables, and the Prutenic Tables. This would deepen the understanding of the Globe's astronomical content and its alignment with contemporary knowledge. Additional studies comparing similar globes from the same period could also reveal systematic production patterns. With heritage preservation in mind, periodic re-digitization will be a means to monitor structural changes over time and support preventive conservation. Finally, in view of outreach applications, digitally reconstructing lost components – such as the stand, hour circle, and other typical components – would enable a more complete and functional virtual representation. Ultimately, this project illustrates how digital modelling can unlock new interdisciplinary insights, minimize physical intervention, and ensure lasting, sustainable access to cultural heritage. The Schissler Globe serves as a compelling case of how 3D digitization can broadly benefit scientific heritage objects by fostering interdisciplinary research and promoting sustainable, accessible preservation.

## Acknowledgements

This work was supported by the Portuguese Fundação para a Ciência e Tecnologia, FCT, I.P./MCTES through national funds: 2020.02581.CEECIND; (PIDDAC): LA/P/0068/2020 (<https://doi.org/10.54499/LA/P/0068/2020>), UID/50019/2025, (<https://doi.org/10.54499/UID/PRR/50019/2025>), UID/PRR2/50019/2025 (<https://doi.org/10.54499/UID/PRR2/50019/2025>), LIBPhys-UNL (<https://doi.org/10.54499/UID/04559/2025>); CIUHCT: UID/00286/2025 (<https://doi.org/10.54499/UID/00286/2025>). Palácio Nacional de Sintra, Parques de Sintra - Monte da Lua, S.A.

## REFERENCES

1. Ramos Carrillo, A.; Moreno Toral, E.; Ruiz Altaba, R., 'Historical-scientific heritage and the university: the two pillars of the History of Pharmacy collection in the Faculty of Pharmacy of the University of Seville', *Conservar Património* **45** (2024) 36-49, <https://doi.org/10.14568/cp28835>.
2. Suay-Matallana, I., 'The material culture of the customs laboratory of Lisbon', *Conservar Património* **30** (2019) 131-139, <https://doi.org/10.14568/cp2018001>.
3. Lourenço, M. C.; Wilson, L., 'Scientific heritage: reflections on its nature and new approaches to preservation, study and access', *Studies in History and Philosophy of Science Part A* **44**(4) (2013) 744-753, <https://doi.org/10.1016/j.shpsa.2013.07.011>.
4. Lourenço, M. C. (ed.), *O Laboratório químico da Escola Politécnica de Lisboa. História, coleções, conservação e musealização*, Museus da Universidade de Lisboa, Lisboa (2013).
5. Magnolo, S.; Galán-Pérez, A., 'Theoretical perspectives: sociology and the conservation of scientific heritage', *Frontiers in Sociology* **9** (2024), <https://doi.org/10.3389/fsoc.2024.1473206>.
6. Schröter, J.; Foasso, C.; Bellot-Gurlet, L.; Brambilla, L., 'Investigating five totalizing counters manufactured by the Alphonse Darras company of the CNAM collections in Paris', *Conservar Património* **44** (2023) 90-102, <https://doi.org/10.14568/cp29230>.
7. Lourenço, M. C.; Gessner, S., 'Documenting collections: cornerstones for more history of science in museums', *Science & Education* **23** (2014) 727-745, <https://doi.org/10.1007/s11191-012-9568-z>.
8. Aguila, E.; Vargiolu, R.; Zahouani, H., 'Étude de l'usure des mécanismes d'horlogerie antiques : application à la restauration du «Tellurium» (1819)', poster, 28<sup>èmes</sup> Journées Internationales Francophones de Tribologie (JIFT), École Nationale d'Ingénieurs de Saint-Etienne (2016), <https://jift2016.sciencesconf.org/100810.html> (accessed 2018-10-14).
9. Tissot, I.; Manso, M., 'Industrial heritage: new paradigms for new conservation challenges', in *Current approaches, solutions and practices in conservation of Cultural Heritage*, eds. G. Emre, A. Yilmaz, P. Pogliani, G. Ildiz & R. Fausto, Istanbul University Press, Istanbul (2024) 159-176, <https://doi.org/10.26650/B/AA9PS34.2024.006.008>.
10. Caleca, M.; Mejía Muñoz, N.; Pollak, E.; Rodriguez Plassa, A., 'The sounds of Jean Tinguely: acoustic imaging as a tool for the kinetic art conservation', student report, Worcester Polytechnic Institute, Zurich (2023), [https://digital.wpi.edu/concern/student\\_works/pr76f771d](https://digital.wpi.edu/concern/student_works/pr76f771d) (accessed 2026-03).
11. Hess, A., 'Authenticity, alterations and museum objects: A close encounter with 2LO, the BBC's first radio transmitter', *Journal of Material Culture* **22**(3) (2017) 281-298, <https://doi.org/10.1177/1359183517702685>.
12. Lemos, M.; Tissot, I., 'Reflection on the conservation challenges of scientific and technological objects', *Conservar Património* **33** (2020) 24-31, <https://doi.org/10.14568/cp2018044>.
13. Agosto, E.; Bornaz, L., '3D models in cultural heritage: approaches for their creation and use', *International Journal of Computational Methods in Heritage Science* **1**(1) (2017) 1-9, <https://doi.org/10.4018/IJCMHS.2017010101>.
14. Lanteri, L.; Calandra, S.; Briani, F.; Germinario, C.; Izzo, F.; Pagano, S.; Pelosi, C.; Santo, A. P., '3D photogrammetric survey, raking light photography and mapping of degradation phenomena of the early renaissance wall paintings by Saturnino Gatti – case study of the St. Panfilo Church in Tornimparte (L'Aquila, Italy)', *Applied Sciences* **13**(9) (2023) 5689, <https://doi.org/10.3390/app13095689>.
15. Acke, L.; De Vis, K.; Verwulgen, S.; Verlinden, J., 'Survey and literature study to provide insights on the application of 3D technologies in objects conservation and restoration', *Journal of Cultural Heritage* **49** (2021) 272-288, <https://doi.org/10.1016/j.culher.2020.12.003>.
16. Makris, D.; Sakellariou, C.; Karampinis, L., 'Emerging materiality through dynamic digital conservation', *Digital Applications in Archaeology and Cultural Heritage* **23** (2021) e00198, <https://doi.org/10.1016/j.daach.2021.e00198>.
17. Bobinger, M., *Schissler der Ältere und der Jüngere* (Schwäbische Geschichtsquellen und Forschungen **5**), Verlag Die Brigg, Augsburg/Basel (1954).
18. Estácio dos Reis, A., 'The oldest existing globe in Portugal', *Der Globusfreund. Wissenschaftliche Zeitschrift für Globen- und Instrumentenkunde* **38** (1990) 57-65.
19. Estácio dos Reis, A., 'Old globes in Portugal', *Separata. Boletim da Biblioteca da Universidade de Coimbra* **42** (1994) 281-298.
20. Gessner, S., 'The Vopelius-Schissler connection: transmission of knowledge for the design of celestial globes in the 16th century', *Bulletin of the Scientific Instrument Society* **104** (2010) 32-42.
21. Gessner, S., '«Geometricus et astronomicus faber». Chr. Schissler aus Augsburg als Hersteller eines wenig bekannten großen Himmelsglobus (1575)', in *Weiter sehen. Beiträge zur Frühgeschichte des Fernrohrs und zur Wissenschaftsgeschichte Augsburgs*, eds. J. Hamel & M. Korey, Acta Historica Astronomiae, Frankfurt a. M. (2012), 123-154.
22. Gessner, S.; Mesquita e Carmo, A., 'Le globe céleste de Schissler: enjeux simultanés d'histoire des sciences et de préservation du patrimoine', in *Proceedings of the International Council of Museums (ICOM), ICOM-CC 16th Triennial Conference, Critério - Produção Gráfica*, Lisboa (2011).

23. Agisoft Metashape (software), <https://www.agisoft.com/> (accessed 2025-05-20).
24. Adobe Photoshop (software), <https://www.adobe.com/products/photoshop.html> (accessed 2025-05-20).
25. CloudCompare (version 2.13 alpha) [GPL software], <http://www.cloudcompare.org/> (accessed 2025-05-20).
26. Matlab 2024a (software), <https://www.mathworks.com/> (accessed 2025-05-20).
27. Toomer, G. J. (trans.), *Ptolemy's Almagest*, Gerald Duckworth, London (1984).
28. Copernicus, N., *De Revolutionibus Orbium Caelestium, Libri VI*, Petreius, Nuremberg (1543).
29. Peters, C. H. F.; Knobel, E. B., *Ptolemy's catalogue of stars: a revision of the Almagest*, Carnegie Institution of Washington, Washington, D.C. (1915).
30. Dekker, E., 'Conspicuous features on sixteenth century celestial globes', *Der Globusfreund. Wissenschaftliche Zeitschrift für Globen- und Instrumentenkunde* **43-44** (1995) 77-97.
31. ArcGIS online, <https://www.arcgis.com/> (accessed 2025-05-20).

RECEIVED: 2025.6.29

REVISED: 2025.7.1

ACCEPTED: 2026.1.29

ONLINE: 2026.6.3



This work is licensed under the Creative Commons Attribution-NonCommercial-NoDerivatives 4.0 International License. To view a copy of this license, visit <http://creativecommons.org/licenses/by-nc-nd/4.0/deed.en>.